AGU PUBLICATIONS

Water Resources Research

RESEARCH ARTICLE

10.1002/2013WR015065

Single-parameter model of vegetated aquatic flows

Ilenia Battiato[1] and Simonetta Rubol[2,3]

[1]Department of Mechanical Engineering, San Diego State University, San Diego, California, USA, [2]Department of Civil, Environmental, and Mechanical Engineering, University of Trento, Trento, Italy, [3]Department of Civil and Environmental Engineering, Duke University, Durham, North Carolina, USA

Key Points:
- Analytical model characterized by one fitting parameter
- Velocities in the canopy and surface layers follow two different scaling laws
- Good agreement between model predictions and experimental data

Correspondence to:
I. Battiato,
ibattiat@gmail.com

Citation:
Battiato, I., and S. Rubol (2014), Single-parameter model of vegetated aquatic flows, *Water Resour. Res.*, *50*, doi:10.1002/2013WR015065.

Received 18 NOV 2013
Accepted 9 JUL 2014
Accepted article online 12 JUL 2014

Abstract Coupled flows through and over permeable layers occur in a variety of natural phenomena including turbulent flows over submerged vegetation. In this work, we employ a two-domain approach to model flow through and over submerged canopies. The model, amenable of a closed-form solution, couples the *log-law* and the Darcy-Brinkman equation, and is characterized by a novel representation of the drag force which does not rely on a parametrization through an unknown drag coefficient. This approach limits to one, i.e., the obstruction permeability, the number of free parameters. Analytical expressions for the average velocity profile through and above the canopies, volumetric flow rate, penetration length, and canopy shear layer parameter are obtained in terms of the canopy layer effective permeability. The model suggests that appropriately rescaled velocities in the canopy and surface layers follow two different scaling laws. The analytical predictions match with the experimental data collected by Ghisalberti and Nepf (2004) and Nepf et al. (2007).

1. Introduction

Submerged vegetation plays a pivotal role in regulating flow and transport in fresh- and sea-water systems. Canopies provide essential ecosystem service: they offer protection to fishes and microinvertebrates and improve the stability of riverbanks by increasing the roughness of the riverbed and decreasing the shear stress which controls erosion and sediment transport [e.g., *Kothyari et al*., 2009; *Nepf*, 2012; *Peruzzo et al*., 2013]. Accurate modeling of the velocity profile within and above the canopies is not only crucial in determining the nutrient dynamics, but also in designing vegetated channels and wetlands, which possess important ecological [e.g., *Ostendorp et al*., 2008; *Mitsch and Gosselink*, 1986], environmental [e.g., *Istanbulluoglu*, 2005], and socioeconomic functions [e.g., *Costanza et al*., 1997; *Katul et al*., 2011]. Yet, modeling of such complex systems has proven to be a formidable task.

A plethora of modelling approaches, both empirical and theoretical, have spurred in the past decades to describe vegetated channel flows. They include phenomenological models based on scale analysis [e.g., *Ghisalberti and Nepf*, 2002; *Huthoff et al*., 2007; *Katul et al*., 2011; *Konings et al*., 2012], momentum balance equations derived from double-averaging methods [e.g., *Ghisalberti and Nepf*, 2004], multiple-domain approaches [e.g., *Nepf and Vivoni*, 2000; *Hsieh and Shiu*, 2006; *Huai et al*., 2009], and their combinations [e.g., *Lowe et al*., 2008; *Poggi et al*., 2009]. We refer to *Nepf and Ghisalberti* [2008] and *Nepf* [2012] for thorough reviews on the topic. While empirical approaches offer simple relationships between relevant quantities (e.g., vegetation-resistance laws), they suffer from an intrinsic lack of generality, as their applicability is limited to the physical conditions in which such models were originally developed. On the other hand, theoretical approaches (derived from balance laws of continuum mechanics) gain in robustness to the detriment of simplicity. They are based on Reynolds equations for turbulent transport which require (first or higher order) closure schemes. The latter can achieve a high degree of sophistication, such as the k-ω and k-ε formulations [e.g., *López and García*, 2001], compared to their first-order counterparts, e.g., eddy viscosity hypothesis and mixing length approaches [e.g., *Poggi et al*., 2009]. Yet, experimental evidence of universal scaling laws suggests that "simple" models may be appropriate to capture the main dynamical features of such multiscale systems [*Ghisalberti*, 2009; *Papke and Battiato*, 2013].

In this letter, we propose a parsimonious (single calibration-parameter) self-consistent two-domain framework to describe turbulent flow in a vegetated open channel. The model, which couples the Darcy-

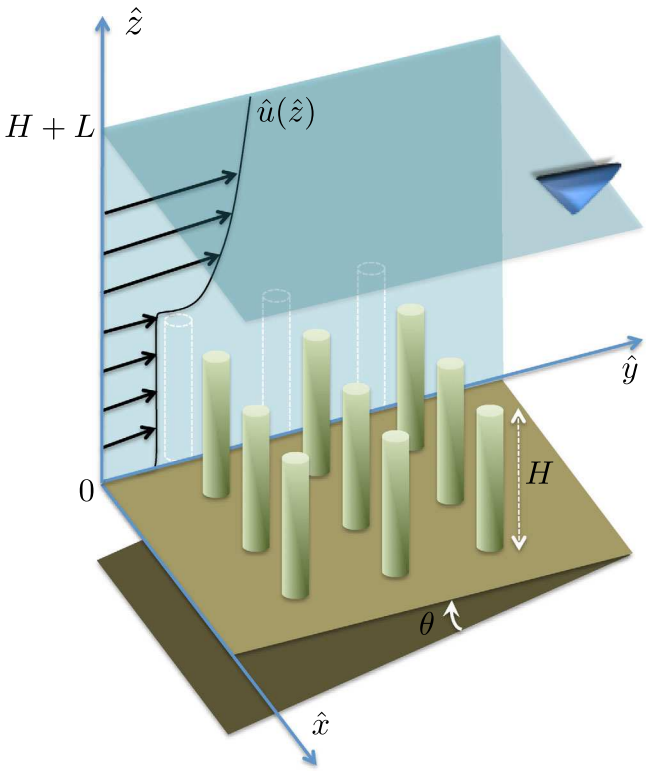

Figure 1. Sketch of fully developed turbulent flow through, $\hat{z} \in (0, H)$, and above, $\hat{z} \in (H, H+L)$, rigid canopies in an open channel of slope θ. A qualitative sketch of the mean velocity profile $\hat{u}(\hat{z})$ is also provided (solid back line).

Brinkman equation with the *log-law* for the flow through and above rigid vegetation, is amenable of a closed-form solution for the mean velocity profile and a number of relevant flow parameters, e.g., volumetric discharge, penetration length, canopy shear layer parameter, and friction factor (section 2). In section 3, we show that appropriately rescaled velocities in the surface and canopy layers follow two different universal scaling behaviors and we compare the model predictions with experimental data collected by *Ghisalberti and Nepf* [2004] and *Nepf et al*. [2007]. Finally, we summarize our results in section 4.

2. Model Formulation

2.1. Two Domain Approach

We consider a two-dimensional fully developed incompressible turbulent flow in an open channel of total height $H + L$ and slope θ, such that $S_0 := \tan\theta \approx \sin\theta$. The upper part of the flow domain, $\hat{z} \in (H, H+L)$, consists of a nonvegetated surface layer of thickness L, while the bottom part of the channel, $\hat{z} \in (0, H)$, is occupied by rigid canopies, referred to as the canopy layer (see Figure 1). We model the latter as a porous medium of permeability K [e.g., *Hsieh and Shiu*, 2006]. Such an approach has proven successful in modeling flows above obstructions for a variety of systems at different scales [e.g., *Battiato et al*., 2010; *Battiato*, 2012; *Papke and Battiato*, 2013].

Two main approaches can be used to couple flow over and through permeable layers: single- and multiple-domain approaches. While the former represents the system with a single domain with nonconstant effective parameters, the latter employs different mathematical models in each subdomain and enforces appropriate boundary conditions at shared interfaces. Here, we employ a two-domain approach and couple the logarithmic mean velocity profile, or *log law*, with a porous medium equation to model the coupled flow above and within the canopies [e.g., *Ghisalberti and Nepf*, 2009]. Although such an approach cannot capture the stem-scale turbulence, it has been largely employed since it allows one (i) to quantify the average flow and the momentum transfer, which regulates biogeochemical processes in the vegetated region, and (ii) to potentially describe arbitrarily complex geometries with a limited number of parameters [*Lowe et al*., 2008, and references therein]. The main novelty of the proposed model, compared to existing ones, lies in its representation of the drag force and in its parametrization, which limit to one (i.e., the obstruction permeability) the number of free parameters.

In the surface layer, the mean velocity in the direction parallel to the channel bottom, $\hat{u}(\hat{z})$, is commonly described by one (of the many) variant of the log law [*Stephan and Gutknecht*, 2002]:

$$\hat{u}(\hat{z}) = \hat{U} + \frac{\hat{u}_\tau}{\kappa} \ln\left(\frac{\hat{z}}{H}\right), \quad \hat{z} \in (H, H+L). \tag{1}$$

In (1), $\kappa = 0.19$ is the reduced von Kármán constant for vegetated channels [*Franca et al*., 2008], $\hat{U}$ is the (mean) velocity at the top of the canopies, and $\hat{u}_\tau$ is the friction velocity. The value of von Kármán coefficient has undergone, and is still undergoing, intense scientific scrutiny both in smooth-wall flows,

atmospheric boundary layers and vegetated flows [e.g., *Leonardi and Castro*, 2010, and references therein]. Some authors go no further than stating that there is no compelling evidence that κ is flow independent. However, there seems to be consensus that in atmospheric boundary layers and flows above permeable layers κ is measurably lower than the smooth-wall value. For dense canopies, the measured Kármán constant are included in the range of 0.16–0.19 [*Kubrak et al.*, 2008]. The friction velocity is defined in terms of the stress at the interface between the free and filtration flow, $\hat{\tau}(H^+)$:

$$\hat{u}_\tau := \sqrt{\hat{\tau}(H^+)/\rho}. \tag{2}$$

An estimate of $\hat{\tau}(H^+)$ can be obtained from Reynolds equation for the fully developed turbulent flow above the canopies,

$$\mathrm{d}_{\hat{z}}\hat{\tau} + \rho g S_0 = 0, \quad \hat{z} \in (H, H+L), \tag{3a}$$

where

$$\hat{\tau}(\hat{z}) := \mu \mathrm{d}_{\hat{z}}\hat{u} - \rho\langle \hat{u}'\hat{v}'\rangle, \quad \hat{z} \in (H, H+L), \tag{3b}$$

is the total shear stress, g, μ, and ρ are the gravitational acceleration, the fluid dynamic viscosity, and density, respectively. In (3b), $\hat{u}'$ and $\hat{v}'$ represent the velocity fluctuations about their respective mean, and $\langle \hat{u}'\hat{v}'\rangle$ is the Reynolds stress. We employ a turbulent viscosity hypothesis to close (3), i.e., $\langle \hat{u}'\hat{v}'\rangle = -v_t(\hat{z})\mathrm{d}_{\hat{z}}\hat{u}$, where v_t is the eddy viscosity [e.g., *Ghisalberti and Nepf*, 2004; *Poggi et al.*, 2009]. Inserting the former into (3b) gives

$$\hat{\tau}(\hat{z}) = \mu_T(\hat{z})\mathrm{d}_{\hat{z}}\hat{u}, \tag{4}$$

where $\mu_T := \mu + \rho v_t(\hat{z}), \hat{z} \in (H, H+L)$. Integrating (3a) from $\hat{z}=H$ to $\hat{z}=H+L$, while accounting for the zero shear condition at the free surface, $\hat{\tau}(H+L)=0$, yields

$$\hat{\tau}(H^+) = \rho g S_0 L. \tag{5}$$

Combining (5) and (2), gives

$$\hat{u}_\tau = \sqrt{g S_0 L}. \tag{6}$$

Consistency between the *log law* (1) where $\hat{u}_\tau$ is given by (6), and the turbulent viscosity hypothesis (4) requires that, at $\hat{z}=H$,

$$\mu_T(H^+)\mathrm{d}_{\hat{z}}\hat{u}|_{H^+} = \rho g S_0 L, \tag{7}$$

where $\hat{u}$ is defined by (1). This yields to

$$\mu_T(H^+) = \rho \kappa H \hat{u}_\tau, \tag{8}$$

which provides a self-consistent estimate of μ_T at the interface between the free and vegetated flows.

Inside the canopies, we employ the Darcy-Brinkman equation for the horizontal component of the intrinsic mean velocity $\hat{u}(\hat{z})$ [e.g., *Stephan and Gutknecht*, 2002; *Katul et al.*, 2011],

$$\mu_e \mathrm{d}_{\hat{z}\hat{z}}\hat{u} - \mu_e K^{-1}\hat{u} + \rho g S_0 = 0, \quad \hat{z} \in (0, H) \tag{9}$$

where K (L^2) is the canopy permeability and μ_e is the fluid "effective" viscosity, respectively. Guided by experimental evidence [e.g., *Ghisalberti and Nepf*, 2004; *White and Nepf*, 2007; *Poggi et al.*, 2009], equation (9) is subject to the no shear condition at $\hat{z}=0$, and the continuity of velocity and shear stress at the interface, $\hat{z}=H$, between the free and obstructed flows [e.g., *Katul et al.*, 2011],

$$\hat{\tau}(0)=0,\ \hat{u}(H^-)=\hat{u}(H^+)=\hat{U},\ \mu_e \mathrm{d}_{\hat{z}}\hat{u}|_{H^-} = \mu_T(H^+)\mathrm{d}_{\hat{z}}\hat{u}|_{H^+}. \tag{10}$$

While not strictly accurate in proximity of the soil layer [*Huai et al.*, 2009], a free shear condition has proved successful in describing the mean velocity profile in most of the canopy layer [e.g. *Ghisalberti and Nepf*, 2004; *White and Nepf*, 2007; *Poggi et al.*, 2009]. A more accurate evaluation of shear stress at the bed can be implemented considering a three layer approach [e.g., *Huai et al.*, 2009]. Since

experimental data suggest smoothness of the mean velocity profile at the interface, we set the effective viscosity equal to the turbulent viscosity at the interface between free and filtration flows, i.e., $\mu_e := \mu_T(H^+)$ in (9) [*Katul et al*., 2011; *Papke and Battiato*, 2013]. Equation (9), which accounts for the viscous and turbulent stresses, the canopy drag and the gravity potential (first, second and third term, respectively), is equivalent to a double-averaged streamwise momentum equation [*Nepf*, 2012, equation (2)], where unsteady and dispersive stress effects have been neglected, as justified by the findings of *Poggi et al*. [2004]. Yet, unlike other models [*Nepf*, 2012, and references therein], where the canopy drag is generally parametrized through a (unknown) drag coefficient, we model the former as a Darcy-type resistance and indirectly account for the turbulence at the canopy scale by including μ_e $(:=\mu_T)$ in the canopy drag term. The first term in (9), where an eddy viscosity closure assumption is employed, is consistent with former formulations of the total stresses [e.g., *Hsieh and Shiu*, 2006; *Nepf*, 2012]. We emphasize that, despite μ_e is assumed constant, the viscous term becomes negligibly small "deeply" inside the canopies, i.e., $\hat{z} \approx (0, \sqrt{K})$, due to the singular nature of Darcy-Brinkman equation in the low-permeability limit.

Choosing the height of the canopies, H, the effective viscosity μ_e and the velocity scale $q = \rho g S_0 H^2/\mu_e$ as repeating variables, (9) can be cast in dimensionless form

$$\mathrm{d}_{zz}u - \lambda^2 u + 1 = 0, \quad z \in (0,1), \tag{11}$$

subject to $\tau(0)=0, u(1^-)=U$, and $\mathrm{d}_z u|_{1^-} = \delta$, where $z=\hat{z}H^{-1}, u=\hat{u}q^{-1}, \delta = LH^{-1}, U=\hat{U}q^{-1}, \lambda^2 = H^2K^{-1}$. The analytical solution of (11) for the mean velocity profile $u(z)$ inside the vegetated layer $z \in [0,1]$ is

$$u(z) = \lambda^{-2} + C(e^{\lambda z} + e^{-\lambda z}), \tag{12a}$$

$$C = \frac{1}{2}\delta\lambda^{-1}\mathrm{csch}\lambda \tag{12b}$$

The interfacial velocity, $U := u(1)$, and the velocity deep inside the canopy (or Darcy velocity), $U_d := u(0)$, are given by

$$U = \lambda^{-2} + \delta\lambda^{-1}\coth\lambda, \tag{13}$$

$$U_d = \lambda^{-2} + \delta\lambda^{-1}\mathrm{csch}\lambda, \tag{14}$$

respectively. We emphasize that (13) (or (14)) provides an operational way of estimating the canopy layer permeability, λ, based on measurements of interfacial (or Darcy) velocity only, once the geometrical features of the channel (S_0 and L) and the height of the canopy layer (H) are determined. Above the canopy layer, the dimensionless *log law* holds:

$$u(z) = U + \delta \ln z, \quad z \in (1, 1+\delta). \tag{15}$$

since $u_\tau := \hat{u}_\tau/q = \kappa\delta$ from the definition of q.

The dimensionless shear stress $\tau := \hat{\tau}H/(\mu_e q) = \mathrm{d}_y u$ can be readily determined from (12)–(15) as

$$\tau(z) = \lambda C(e^{\lambda z} - e^{-\lambda z}), \quad z \in (0, 1^-), \tag{16a}$$

$$\tau(z) = \delta z^{-1}, \quad z \in (1^+, 1+\delta). \tag{16b}$$

Figure 2 plots $u(z)$ and $\tau(z)$ for different values of $\lambda \geq 1$. As permeability decreases (or λ increases), the flow profile inside the obstruction becomes progressively more uniform and the shear stress decreases quickly to zero within the porous layer.

In the following, we provide analytical expressions for a number of relevant quantities, generally employed to characterize flows in vegetated channels, e.g., volumetric discharge, penetration length, drag length scale, canopy shear layer parameter, and the friction factor.

2.2. Analytical Expressions

The closed-form expressions (12) and (15) allow one to analytically determine various quantities, relevant in describing vegetated flows, with no need of additional parametrization. All such quantities can be uniquely determined from the channel geometrical features, once the canopy layer permeability has been estimated (from, e.g., velocity measurements).

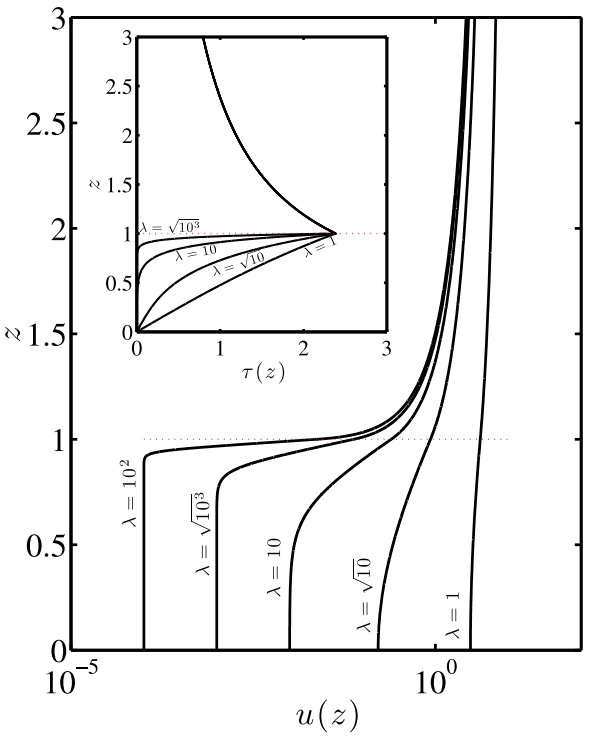

Figure 2. Dimensionless mean velocity $u(z)$ and shear stress $\tau(z)$ (inset) within and above the canopy layer for different values of the dimensionless permeability λ.

2.2.1. Discharge, Bulk Velocity and Friction Factor

The volumetric discharge $\hat{Q}$ [L^3T^{-1}] through a vegetated channel of width $\hat{W}$ [L] can be estimated from integration of the properly rescaled mean velocity profiles within and above the canopy layer (12) and (15), respectively. The dimensionless volumetric discharge per unit width $Q_W := Q/W$, where $Q = \hat{Q}q^{-1}H^{-2}$ and $W = \hat{W}/H$ are the dimensionless volumetric flow rate and channel width, respectively, is given by $Q_W = \int_0^1 [\lambda^{-2} + C(e^{\lambda z} + e^{-\lambda z})]dz + \int_1^{1+\delta} (U + \delta \ln z)dz$. Integration yields to

$$Q_W = \lambda^{-2} + C\lambda^{-1}(e^{\lambda} - e^{-\lambda}) + \delta[(1+\delta)\ln(1+\delta) + U - \delta]. \tag{17}$$

We emphasize that Q_W can be determined solely from canopy attributes, i.e., δ and λ. The bulk velocity $\hat{U}_b$ can be readily calculated as

$$\hat{U}_b = \frac{qQ_W}{1+\delta}. \tag{18}$$

The friction factor f is defined as

$$f := 8\frac{\hat{\tau}(H)}{\rho \hat{U}_b^2}, \tag{19}$$

(i.e., $f := 4C_f$, where C_f is the skin friction coefficient). From (5) and (6), $\hat{\tau}(H) = \rho \hat{u}_\tau^2$. Then, (19) can be rearranged to recover the classical Darcy-Weisbach formula:

$$\frac{\hat{u}_\tau}{\hat{U}_b} = \sqrt{\frac{8}{f}}. \tag{20}$$

2.2.2. Penetration Length

The depth, below the canopy surface, where the stress reaches a fixed (however arbitrary) value of the maximum stress, $\tau_{max} = \hat{\tau}(H)$, is referred to as penetration length $\hat{\delta}_e$. Generally this percentage is fixed at 10% of $\hat{\tau}_{max}$ [*Nepf and Vivoni*, 2000; *Murphy et al.*, 2007; *Ghisalberti*, 2009]. In dimensionless form,

$$\delta_e : \quad \tau(1-\delta_e) = 0.10\tau(1) \tag{21}$$

where $\delta_e := \hat{\delta}_e/H$. Combining (21) with (16a) leads to

$$\delta_e = 1 - \lambda^{-1}\text{asinh}(0.1\sinh\lambda). \tag{22}$$

2.2.3. Drag Length Scale and Canopy Shear Layer

Another relevant parameter is $C_D a$, the product between the medium drag coefficient, C_D, and the frontal area of the canopies per unit volume, a, referred to as the inverse of the drag length scale ($[C_D a] = L^{-1}$). It is defined as

$$C_D a = \frac{2|\hat{F}|}{\rho \hat{U}_c^2}, \tag{23}$$

where $\hat{F}$ is the drag force per unit volume of porous medium, and $\hat{U}_c$ is a characteristic flow velocity, which we set equal to $\hat{U}$ [*Papke and Battiato*, 2013]. Since $\hat{F}(1) = -\mu_e \hat{U}/K$ at the interface of a Brinkman medium and $\hat{\tau}/\tau = \mu_e q/H$ from the definition of dimensionless stress, (23) can be rewritten as

$$C_D a = \frac{2\lambda^2}{H}\frac{U}{\tau(1)}\left(\frac{\hat{u}_\tau}{\hat{U}}\right)^2. \tag{24}$$

As $\tau(1)=\delta$ and $u_\tau=\kappa\delta$, (24) becomes

$$C_D a = \frac{1}{H}\frac{2\delta}{U}(\lambda\kappa)^2, \tag{25}$$

which provides a closed-form expression for $C_D a$ in terms of geometric features of the channel and the interfacial velocity. The canopy shear layer, CSL, is defined in terms of $C_D a$ as

$$\mathrm{CSL} := C_D a \frac{\hat{U}}{\mathrm{d}_{\hat{z}}\hat{u}|_H}. \tag{26}$$

Nepf et al. [2007] showed experimentally that the CSL is statistically independent of the canopy Reynolds' number $Re_h := H\hat{U}/\nu$ for $Re_h \in (10^3, 10^6)$, and its value approximately equal to 0.23 $\pm$0.06. In particular, they proposed, and experimentally supported, the scaling law [*Nepf et al*., 2007, equation (5)],

$$\frac{\hat{\delta}_e}{H} \approx \frac{\mathrm{CSL}}{C_D a H}. \tag{27}$$

In the following, we verify that the proposed model is consistent with the experimental observation by *Nepf et al*. [2007] and with the scaling law (27). Multiplying both sides of (24) by $\hat{U}/(\mathrm{d}_{\hat{z}}\hat{u}|_H)$, yields to

$$\mathrm{CSL} = 2(\lambda\kappa)^2, \tag{28}$$

since $\mathrm{d}_z u|_1 = \tau(1) = \delta$ and $u_\tau = \kappa\delta$. Consistently with data, CSL is independent of Reynolds number. Yet, according to the proposed model, CSL is not a constant among canopy flows characterized by different obstruction permeabilities. For canopy layers of low permeability (i.e. $\lambda \to \infty$), the dimensionless penetration length δ_e scales as

$$\delta_e \sim \lambda^{-1}\ln 10 \tag{29}$$

since $\tau(1) \sim \delta$ and $\tau(1-\delta_e) \sim \delta \mathrm{e}^{-\delta_e\lambda}$. The asymptotic behavior of $C_D aH$ for thin vegetated layers, $\Lambda := \lambda\delta \gg 1$, is

$$C_D aH \sim 2\lambda^3\kappa^2, \tag{30}$$

since $U \sim \delta/\lambda$ when $\Lambda \gg 1$, i.e. it is independent of δ. The asymptotic behavior of CSL, δ_e and $C_D aH$ given by (28), (29), and (30), respectively, suggests that

$$\frac{\mathrm{CSL}}{C_D a \hat{\delta}_e} \approx \mathrm{const}, \tag{31}$$

i.e. the ratio is invariant for thin vegetated layers in the low-permeability limit. This is consistent with (27). In the following, we validate our theoretical predictions against experimental data published elsewhere.

3. Comparison With Experimental Data

We compare our model predictions with the data set collected by *Ghisalberti and Nepf* [2004] and *Nepf et al*. [2007].

Unlike other models, the proposed approach allows one to fully determine the flow response once H, L, S_0, and K are known. Current analytical and semianalytical models contain many additional fitting parameters. For example, concurrent measurements of C_D, a, H, L, S_0, and a momentum absorption coefficient, β, are often required [*Katul et al*., 2011]. The latter can be determined using empirical relationship which contains additional fitting parameters, [*Katul et al*., 2011, equation (19)]. Alternatively, estimates of the mixing length δ_e and other constants [e.g. *Huai et al*., 2009, equation (1)] are necessary beyond C_D, a, H, L, and S_0 values. Other models necessitate of both the zero-plane displacement and the momentum roughness height, or employ empirical relationships for parameter estimation [*Nepf et al*., 2007]. More parsimonious models, which provide estimates of overflow and in-patch depth-averaged velocities, have been

Table 1. Model Parameters

Run	A	B	C	D	E	F	G	H	I	J	K
δ [-]	2.36	2.36	2.36	2.36	2.38	2.38	2.38	2.38	2.38	2.38	2.38
λ [-]	1.60	1.60	1.76	1.76	1.63	1.63	1.63	1.90	1.90	1.90	1.90
Λ [-]	3.78	3.78	4.14	4.14	3.89	3.89	3.89	4.52	4.52	4.52	4.52

proposed [e.g., *Huthoff et al*., 2007; *Yang and Choi*, 2010; *Konings et al*., 2012; *Luhar and Nepf*, 2013]. They generally require a smaller set of fitting parameters, yet they do not provide a vertical distribution of the mean velocity.

Since permeability is a function of the geometrical properties of the array, we assume that model canopies with the same value of a possess the same K (or λ). Therefore, we group the available measurements into four classes of equivalent porous media corresponding to the four values of a, $a=\{0.025, 0.034, 0.040, 0.080\}$.

For each class of porous medium, we calculate K (or λ) from a single measurement of the interfacial velocity in one particular run through (13). Specifically, we employ runs A, C, E, and H to calculate the permeability for each geometrical configuration. The calculated values are $K_A=7.53\cdot10^{-3}\mathrm{m}^2(\lambda_A=1.60)$, $K_C=6.26\cdot10^{-3}\mathrm{m}^2(\lambda_C=1.76)$, $K_E=7.16\cdot10^{-3}\mathrm{m}^2(\lambda_E=1.63)$ and $K_H=5.27\cdot10^{-3}\mathrm{m}^2(\lambda_H=1.90)$ for runs A, C, E, and H, respectively. After calculating permeability, we perform a parameter-free prediction on available quantities (e.g. $\hat{U}, \hat{U}_d$, and $\hat{Q}$) for the same and remaining runs. A list of dimensional and dimensionless model parameters, including the fitted values of K (or λ), is provided in Table 1. We emphasize that there are a number of alternative options to estimate permeability K (or λ). These include (i) drag coefficient measurements or estimates (e.g., $C_D\approx1$) which can be linked to λ through (25) or (30); (ii) velocity measurements at arbitrary locations in the flow field, e.g., the velocity deep inside the canopy or any velocity measurements in the surface layer; (iii) prediction from geometric information of the canopy layer, i.e. porosity ϕ and stem density a (obtained from remote sensing or lidar data) through either (semi-)empirical, analytical, or numerical models [e.g., *Sobera and Kleijn*, 2006; *Mattis et al*., 2012, and references therein].

Figure 3a shows a comparison between the measured interfacial velocity $\hat{U}$ and the model prediction provided by (13) for runs B, D, F, G, I, J, and K. We emphasize that, for the previous runs, the prediction is parameter free. Similarly, Figure 3b presents a comparison between the velocity deep inside the canopy (or Darcy velocity) as predicted by the model and the measured values for all the runs. Figure 3c compares the experimentally determined volumetric discharge $\hat{Q}$ and its prediction through (17) for each run. The predicted values are generally in good agreement with the experimental data. The discrepancy between the predicted and measured volumetric flow rate for low values of discharge is to be expected. The *log law* employed to compute $\hat{Q}$ is not valid in proximity of the surface where a free shear condition should

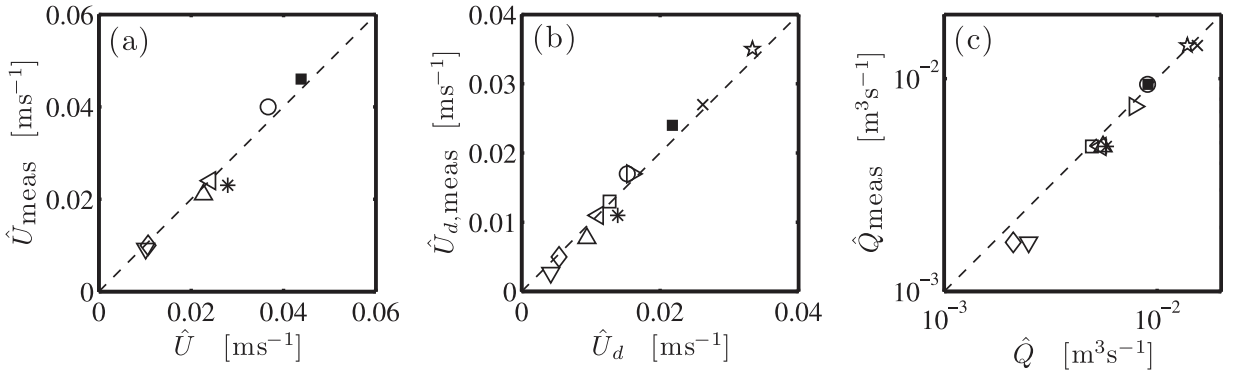

Figure 3. Comparison between measured and predicted (a) interfacial velocity $\hat{U}$, (b) velocity deep inside the canopies $\hat{U}_d$, and (c) volumetric discharge $\hat{Q}$ for runs A (square), B (diamond), C (right-pointing triangle), D (left-pointing triangle), E (star), F (black square), G (asterisk), H (cross), I (circle), J (triangle), and K (inverted triangle). Figure 3a does not include the runs used for fitting, i.e. runs A, C, E, and H. The line 1:1 is showed.

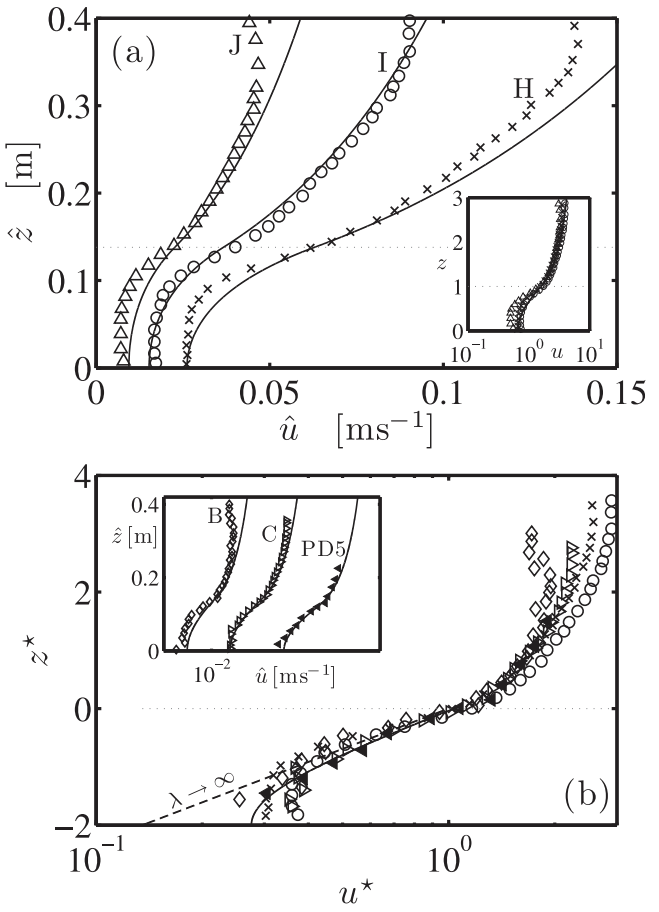

Figure 4. (a) Comparison between experimental velocity measurements (points) and model predictions (solid lines) for runs H, I, and J. The permeability value K (or λ) for the three configurations is obtained through a one-point fitting of the interfacial velocity $\hat{U}$ for run H by means of (13). The fitted value of λ (≈ 1.90) is then employed to perform a pure prediction on the remaining data set. The inset shows a plot of $u(z)$ (solid line) and the appropriately rescaled data. It supports the model assumption that canopy layers with the same stem density, as for runs H, I, and J, have the same permeability. (b) Rescaled data (according (32)) for velocity profiles B, C, H, I, J, and PD5 [*Katul et al.*, 2011], corresponding to canopy layers with different permeabilities. The main figure shows that the asymptotic limit for $\lambda \to \infty$ (dashed line) is not fully reached, since $\lambda \approx 2$ (solid line) for the data set considered here. The nonrescaled data corresponding to runs B, C, and PD5 and the model predictions (solid lines) are presented in the inset.

be satisfied; this leads to overestimate the velocity profile close to the free surface, and consequently the total discharge. This effect becomes more noticeable for low values of discharge, where such overestimate constitutes a higher percentage of the total discharge.

The CSL parameter can be promptly estimated through (28). The analytical predictions of CSL corresponding to the minimum and maximum values of λ among all the runs are CSL ≈ 0.19 and CSL ≈ 0.26 for λ=1.6 and λ=1.9, respectively. These results are in excellent agreement with the experimental mean value of 0.23 and a standard deviation between all measurements of 0.06 [*Nepf et al.*, 2007, Figure 2]. Our theoretical result suggests that the scatter between the different sets of data may be attributed to different values of permeabilities between the canopy layers. The analytical solution well compares with the experimental data.

Given the obstruction permeability and the geometric features of the channel, the mean velocity profile is uniquely determined by (12)–(15). Figure 4a compares the experimental measurements and the simulated dimensional mean velocity profiles for runs H, I, and J. We emphasize that the analytical predictions for runs I and J are parameter free. The results indicate the model is able to successfully reproduce the velocity profile except in proximity of the free interface where the *log law* is invalid. The inset in Figure 4a, which plots the dimensionless velocity profile (12a) and the correspondingly rescaled data, supports the hypothesis that arrays with equal stem density a possess the same permeability and exhibit a similar dynamical response, if appropriately rescaled.

For canopy layers of different permeabilities, we seek dynamic similarity by investigating the asymptotic behavior of (12) in the low-permeability limit, i.e. $\lambda \to +\infty$ [*Battiato*, 2012; *Papke and Battiato*, 2013]. Since $C \sim \delta\lambda^{-1}\mathrm{e}^{-\lambda}$, we can define

$$u^\star := \frac{u(y^\star/\lambda;\lambda)-\lambda^{-2}}{\lambda/\delta} \tag{32}$$

whose asymptotic behavior $u^\star \sim \mathrm{e}^{y^\star}$ is independent of λ, where $y^\star=\lambda(z-1)$ and $y^\star \in (-\lambda, 0)$. Figure 4b plots rescaled data (according (32)) for velocity profiles B, C, H, I, J, and PD5 [*Katul et al.*, 2011]. As $\lambda \approx 2$ (solid line) for the data set considered here, the asymptotic limit for $\lambda \to \infty$ (dashed line) is not fully

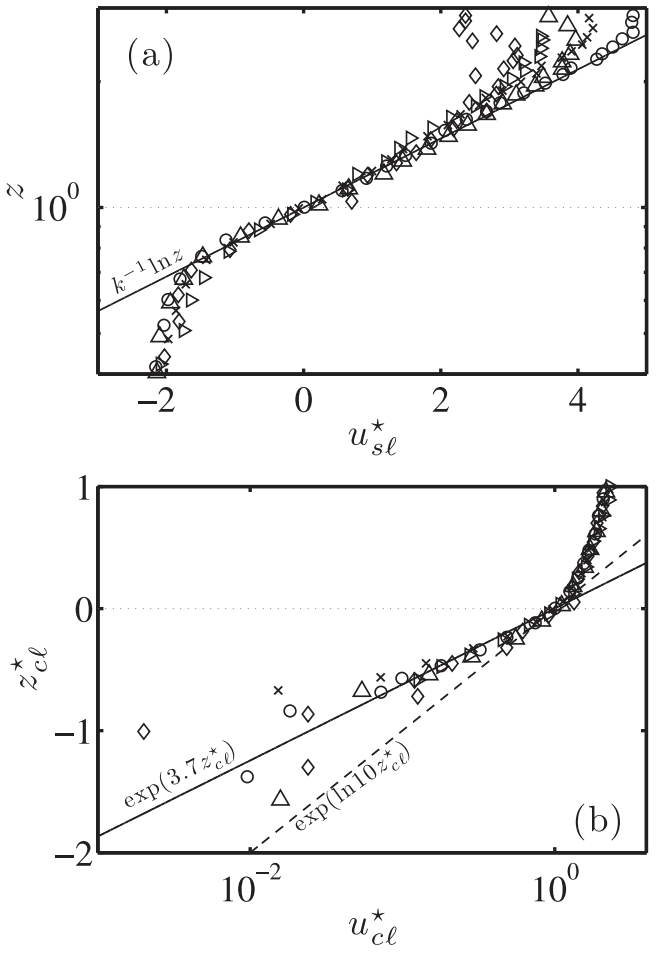

Figure 5. (a) Rescaled velocity data $u^\star_{s\ell} := (\hat{u}-\hat{U})/\hat{u}_\tau$ versus $z=\hat{z}/H$ for runs B, C, H, I, and J. The data in the surface layer collapse onto the theoretical prediction, $u^\star_{s\ell}=\kappa^{-1}\ln z$ (solid line); (b) Rescaled velocity data $u^\star_{c\ell} := (\hat{u}-\hat{U}_d)/(\hat{U}-\hat{U}_d)$ versus $z^\star_{c\ell} := (\hat{z}-H)/\hat{\delta}_e$. The rescaled data follow the theoretical scaling $u^\star_{c\ell} \sim \exp(cz^\star_{c\ell})$, with $c \approx 3.7$ (solid line), yet they deviate from the theoretical prediction $u^\star_{c\ell} \sim \exp(\ln 10 z^\star_{c\ell})$ valid in the limit $\lambda \to +\infty$ (dashed line). This is to be expected since all the runs are characterized by $\lambda \approx 2$.

reached, as apparent from the λ-dependent tails deviating from (32). The nonrescaled data for runs B, C, and PD5 and the model predictions (solid lines) are presented in the inset of Figure 4b.

It is worth noticing that (15) and (32) suggest that two different velocity scalings exist in the surface and canopy layers, respectively. In particular, (15) gives

$$u^\star_{s\ell} := \frac{\hat{u}-\hat{U}}{\hat{u}_\tau} = \kappa^{-1}\ln z \qquad (33)$$

with $z=\hat{z}/H$, i.e. $u^\star_{s\ell}$ is a universal function in the surface layer, $z>1$. In the canopy layer, combining (29) with (32), while accounting for $U-U_d \sim \lambda\delta^{-1}$ (as $\lambda \to +\infty$), yields to the following scaling

$$u^\star_{c\ell} := \frac{\hat{u}-\hat{U}_d}{\hat{U}-\hat{U}_d} \sim \mathrm{e}^{cz^\star_{c\ell}}, \quad \lambda \to +\infty \qquad (34a)$$

$$z^\star_{c\ell} := \frac{\hat{z}-H}{\hat{\delta}_e}, \qquad (34b)$$

with $c=\ln 10$, i.e. $\ln(u^\star_{c\ell})$ is linearly proportional to $z^\star_{c\ell}$. The previous scalings are similar to those proposed by, e.g., *Katul et al.* [2011, equation (14)]. Although derived under the assumption of free-shear at the channel bed, the universal scaling (34) is independent from the specific boundary condition imposed at the bed surface [*Battiato*, 2012]. The scaling laws (33) and (34) demonstrate that appropriately rescaled quantities become independent of λ (or permeability), as $\lambda \to +\infty$ (or permeability is sufficiently small). This has two direct implications. First, it shows that the space dimension of independent (dimensionless) parameters that fully describe the system dynamics can be reduced from two (δ and λ) to one (δ only). Second, it suggests that appropriately rescaled flow quantities become approximately independent of λ when the former is large enough, i.e. the system response is not strongly sensitive to λ estimates (and/or measuring errors) when permeability is small. In this sense, λ appears as a robust parameter for modeling vegetated flows. Yet, for vegetated conditions where λ is not much larger than one, deviations from (34) may occur. In Figure 5a, we plot the experimental data rescaled according to (33). The data in the surface layer collapse onto the theoretical prediction. In Figure 5b, we rescale the velocity data according to (34). In a semilogarithmic plot, the rescaled velocity data $\ln(u^\star_{c\ell})$ are indeed linearly dependent with the rescaled coordinate system $z^\star_{c\ell}$, with $c \approx 3.7$. Deviations from the theoretical prediction in the limit as $\lambda \to \infty$ are to be expected since $\lambda \approx 2$ for the data set considered.

The ability to estimate canopy layer permeability based solely on geometrical features of the stem arrangement would allow one to predict flow response from geometric information of vegetation acquired, e.g., from remote sensing devises. There are multiple formulas to independently estimate permeability of a porous medium from its geometric features [*Sobera and Kleijn*, 2006, and references therein]. Yet, they are

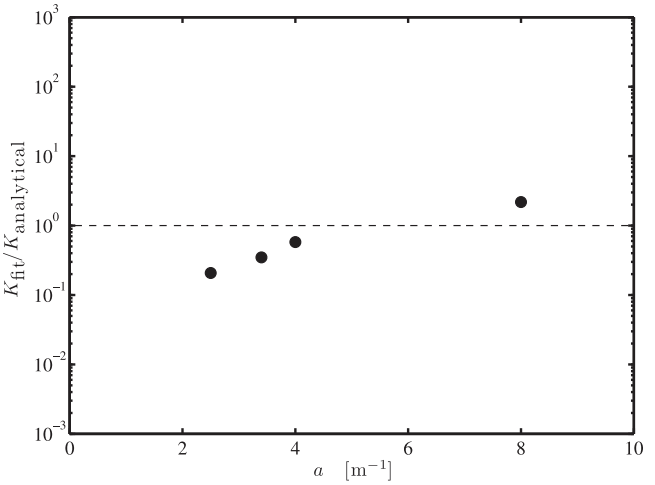

Figure 6. Ratio between the fitted and predicted permeability values for the experimental canopy configurations corresponding to $a = \{2.5, 3.4, 4, 8\}$ m^{-1}. Equation (35) is able to capture the correct order of magnitude of the canopy layer permeability solely from geometric information of the canopy structure, i.e. porosity ϕ and canopy density a.

generally empirical formulas and contain a number of fitting parameters. As such, their applicability is limited to the physical conditions under which they have been derived and they are less accurate than the use of actual velocity data. Much fewer semianalytical approximate formulations are available, except for highly idealized systems. Here, we compare the permeability values as obtained by one-point fitting of velocity data with the analysis proposed by [*Happel*, 1959], which describes the laminar viscous flow through a regular array of infinite cylinders of radius R_0 and half-distance between cylinders R_1 aligned orthogonally to the mean flow direction. The permeability of such an array is given as [*Happel*, 1959, equation (19)]

$$K = R_1^2 f(\phi) \tag{35a}$$

where

$$f(\phi) = \frac{1}{8}\left[-\ln(1-\phi) - \frac{(1-\phi)^{-2}-1}{(1-\phi)^{-2}+1}\right] \tag{35b}$$

and $\phi = 1 - R_0^2/R_1^2$ is the forest porosity. Assuming the stems are arranged in regular arrays, then R_1 can be approximated as $R_1 = 1/(2a)$, where $a = 2nR_0$ and n is the canopy stem density (i.e. number of stems per unit area). While for the experimental runs used in this study, the mean leaf area index (LAI) is not provided, the latter can be related to a through, e.g., LAI $\approx aH$ [*Katul et al.*, 2011]. For the four configurations corresponding to values of $a = \{2.5, 3.4, 4, 8\}$ m^{-1}, we plot the ratio between the fitted and predicted permeability value (see Figure 6). Despite permeability values can span up to 20 orders of magnitude depending on the system under consideration (from 10^{-19}m^2 in "impervious" rocks to 10^{-2}m^2 for highly permeable layers), Figure 6 shows that (35) can predict the correct order of magnitude of the canopy permeability without any fitting parameter, given the canopy density a (or LAI) and the canopy layer porosity ϕ are provided. The discrepancy between the predicted and fitted permeability values is to be expected due to deviations of the experiment from the model approximations and/or highly idealized conditions, which include, e.g., flow steadiness and one-dimensionality, and regular arrangement of stems. Yet, the approach shows promise in its ability to directly link canopy geometry (obtained, e.g., from lidar data) to flow response. Development of more accurate relationships between geometrical features and canopy permeability, to include, e.g. finite height and bending effects in (35), is subject of current research.

4. Conclusions

Turbulent flows above submerged vegetation are ubiquitous in natural systems and their accurate modelling is crucial in determining nutrients dynamics and the hydrodynamic response of wetlands and vegetated channels. We propose a single fitting-parameter model to describe turbulent flow in a densely vegetated open channel. The model couples the Darcy-Brinkman equation with the *log law* for the flow within and above the canopy layer, and employs a first-order closure scheme of the Reynolds equation to provide a self-consistent estimate of the turbulent viscosity at the interface between the canopy and free flow. Further, we model the drag force as a Darcy-type resistance with a modified effective viscosity which

accounts for turbulence at the canopy scale, without relying on a more common parametrization through a (unknown) drag coefficient. The model, amenable of analytical solution for the mean velocity, allows one to determine closed-form expressions for a number of relevant physical quantities, including volumetric discharge, bulk velocity, penetration length, drag length scale, and canopy shear layer parameter (CSL), without relying on additional parametrization. The model results show that the parameters governing the dynamical response of appropriately dimensionless quantities are purely geometric, i.e. a dimensionless canopy layer permeability λ and height δ. This information can directly guide the design of laboratory-scale models which are *dynamically similar* to their corresponding prototypes in natural environments (i.e., at the field-scale). According to the proposed model, dynamic similarity is achieved when λ and δ are kept constant between the model and the prototype. The model suggests that appropriately rescaled velocities in the canopy and surface layers exhibit different scalings laws. The scaling laws show that the space of dimensionless parameters can be further reduced when permeability is very small, i.e. $\lambda \to +\infty$, and the dynamical response of vegetated layers becomes universal. It is worth noticing that the proposed approach, consistent by construction with the framework proposed by *Papke and Battiato* [2013], satisfies also the universal scaling laws experimentally observed by *Ghisalberti* [2009], under appropriate conditions. The model predictions and the proposed scalings compare well with experimental data collected by *Ghisalberti and Nepf* [2004], *Poggi et al.* [2004] and *Nepf et al.* [2007].

While the proposed framework is applicable to rigid and moderately flexible canopies, generalizations to more realistic configurations, e.g. highly flexible and heterogeneous (i.e. with spatially variable permeability) canopy layers, necessitate the coupling of canopy bending and flow field dynamics. This is subject of current investigations together with the application of the proposed model to transport of passive and reactive solutes in vegetated aquatic flows.

Acknowledgments
Ilenia Battiato gratefully acknowledges support by the National Science Foundation under award number EAR-1246297. Simonetta Rubol acknowledges the support of the Provincia Autonoma di Trento and the European Commission. This project has received funding from the European Union's Seventh Framework Programme for research, technological development and demonstration under grant agreement number PCOFUND-GA-2008-226070.

References

Battiato, I. (2012), Self-similarity in coupled Brinkman/Navier-Stokes flows, *J. Fluid Mech.*, *699*, 94–114.
Battiato, I., P. R. Bandaru, and D. M. Tartakovsky (2010), Elastic response of carbon nanotube forests to aerodynamic stresses, *Phys. Rev. Lett.*, *105*, 144504.
Costanza, R., et al. (1997), The value of the world's ecosystem services and natural capital, *Nature*, *387*, 253–260.
Franca, M., R. Ferreira, and U. Lemmin (2008), Parameterization of the logarithmic layer of double-averaged streamwise velocity profiles in gravel-bed river flows, *Adv. Water Resour.*, *31*, 915–925.
Ghisalberti, M. (2009), Obstructed shear flows: Similarities across systems and scales, *J. Fluid Mech.*, *641*, 51–61.
Ghisalberti, M., and H. Nepf (2002), Mixing layers and coherent structures in vegetated aquatic flows, *J. Geophys. Res*, *107*(C2), doi:10.1029/2001JC000871.
Ghisalberti, M., and H. Nepf (2009), Shallow flows over a permeable medium: The hydrodynamics of submerged aquatic canopies, *Transp. Porous Media*, *78*(2), 309–326.
Ghisalberti, M., and H. M. Nepf (2004), The limited growth of vegetated shear layers, *Water Resour. Res.*, *40*, W07502, doi:10.1029/2003WR002776.
Happel, J. (1959), Viscous flow relative to arrays of cylinders, *AIChE J.*, *5*, 174–177.
Hsieh, P.-C., and Y.-S. Shiu (2006), Analytical solutions for water flow passing over a vegetal area, *Adv. Water Resour.*, *29*(9), 1257–1266.
Huai, W., Y. Zeng, Z. Xu, and Z. Yang (2009), Three-layer model for vertical velocity distribution in open channel flow with submerged rigid vegetation, *Adv. Water Resour.*, *32*(4), 487–492.
Huthoff, F., C. Augustijn, and S. Hulscher (2007), Analytical solution of the depth-averaged flow velocity in case of submerged rigid cylindrical vegetation, *Water Resour. Res.*, *43*, W06413, doi:10.1029/2006WR005625.
Istanbulluoglu, E. (2005), Vegetation-modulated landscape evolution: Effects of vegetation on landscape processes, drainage density, and topography, *J. Geophys. Res.*, *110*, F02012, doi:10.1029/2004JF000249.
Katul, G., D. Poggi, and L. Ridolfi (2011), A flow resistance model for assessing the impact of vegetation on flood routing mechanics, *Water Resour. Res.*, *47*, W08533, doi:10.1029/2010WR010278.
Konings, A., G. Katul, and S. Thompson (2012), A phenomenological model for the flow resistance over submerged vegetation, *Water Resour. Res.*, *48*, W02522, doi:10.1029/2011WR011000.
Kothyari, U. C., H. Hashimoto, and K. Hayashi (2009), Effect of tall vegetation on sediment transport by channel flows, *J. Hydraul. Res.*, *47*(6), 700–710.
Kubrak, E., J. Kubrak, and M. R. Rowiński (2008), Vertical velocity distributions through and above submerged, flexible vegetation, *Hydrol. Sci. J.*, *53*(4), 37–41.
Leonardi, S., and I. Castro (2010), Channel flow over large cube roughness: a direct numerical simulation study, *J. Fluid Mech.*, *651*, 519–539.
López, F., and M. García (2001), Mean flow and turbulence structure of open-channel flow through non-emergent vegetation, *J. Hydraul. Eng.*, *127*(5), 392–402.
Lowe, R. J., U. Shavit, J. L. Falter, J. R. Koseff, and S. G. Monismith (2008), Modeling flow in coral communities with and without waves: A synthesis of porous media and canopy flow approaches, *Limnol. Oceanogr.*, *53*(6), 2668–2680.
Luhar, M., and H. M. Nepf (2013), From the blade scale to the reach scale: A characterization of aquatic vegetative drag, *Adv. Water Resour.*, *51*, 305–316.
Mattis, S. A., C. N. Dawson, C. E. Kees, and M. W. Farthing (2012), Numerical modeling of drag for flow through vegetated domains and porous structures, *Adv. Water Resour.*, *39*, 44–59.
Mitsch, W., and J. Gosselink (1986), *Wetlands*, Van Nostrand Reinhold, N. Y.

Murphy, E., M. Ghisalberti, and H. Nepf (2007), Model and laboratory study of dispersion in flows with submerged vegetation, *Water Resour. Res.*, *43*, W05438, doi:10.1029/2006WR005229.
Nepf, H. (2012), Flow and transport in regions with aquatic vegetation, *Annu. Rev. Fluid Mech.*, *44*(1), 123–142.
Nepf, H., and M. Ghisalberti (2008), Flow and transport in channels with submerged vegetation, *Acta Geophys.*, *56*(3), 753–777.
Nepf, H., and E. Vivoni (2000), Flow structure in depth-limited, vegetated flow, *J. Geophys. Res.*, *105*(C12), 28,547–28,557.
Nepf, H., M. Ghisalberti, B. White, and E. Murphy (2007), Retention time and dispersion associated with submerged aquatic canopies, *Water Resour. Res.*, *43*, W04422, doi:10.1029/2006WR005362.
Ostendorp, W., T. Gretler, M. Mainberger, M. Peintinger, and K. Schmieder (2008), Effects of mooring management on submerged vegetation, sediments and macro-invertebrates in Lake Constance, Germany, *Wetl. Ecol. Manag.*, *17*(5), 525–541.
Papke, A., and I. Battiato (2013), A reduced complexity model for dynamic similarity in obstructed shear flows, *Geophys. Res. Lett.*, *40*, 3888–3892, doi:10.1002/grl.50759.
Peruzzo, P., A. Defina, H. M. Nepf, and R. Stocker (2013), Capillary interception of floating particles by surface-piercing vegetation, *Phys. Rev. Lett.*, *111*, 164501.
Poggi, D., A. Porporato, L. Ridolfi, J. D. Albertson, and G. G. Katul (2004), The effect of vegetation density on canopy sublayer turbulence, *Boundary Layer Meteorol.*, *111*(3), 565–587.
Poggi, D., C. Krug, and G. Katul (2009), Hydraulic resistance of submerged rigid vegetation derived from first-order closure models, *Water Resour. Res.*, *45*, W10442, doi:10.1029/2008WR007373.
Sobera, M. P., and C. R. Kleijn (2006), Hydraulic permeability of ordered and disordered single-layer arrays of cylinders, *Phys. Rev. E*, *74*, 036,301.
Stephan, U., and D. Gutknecht (2002), Hydraulic resistance of submerged felixible vegetation, *J. Hydrol.*, *269*, 27–43.
White, B. L., and H. M. Nepf (2007), Shear instability and coherent structures in shallow flow adjacent to a porous layer, *J. Fluid Mech.*, *593*, 1–32.
Yang, W., and S.-U. Choi (2010), A two-layer approach for depth-limited open-channel flows with submerged vegetation, *J. Hydraul. Res.*, *48*(4), 466–475.